Autopoietic Physics: Scaling Quantum Cellular Automata (QCAs) in Archetypal Physical Structures

D.W. Belousek
Dept. of Hist. and Phil. of Science,
Notre Dame University, Notre Dame IN 46556, USA
J.A. Ellis (Phys.), J.K. Ellis (Phys.), E.B. Flint (Chem.),
S. Schulz (Phys.), K.R. Roos*(Phys.), and J.P. Kenny (Phys.),
Bradley University, Peoria, Illinois 61625, U.S.A.

ABSTRACT. A unique cellular automaton, the quantum cellular automaton (QCA), is advanced as a candidate process for describing basic quantum mechanics in real space and real time. The QCA mimics a zitterbewegung motion arising from the Dirac free particle equation for fermions in a confined lattice space-time. It emerges from employing simple QCA calculational rules that a series of scaled autopoietic (self forming) processes can be used to describe diverse states such as atoms, nuclei and elementary particles when scaled in the 3+1 D state. Fractal features associated with the QCA hint at a intimate link between chaos/fractal properties and the fundamental efforts to understand the roots of quantum physics in real space and real time. The QCA describes a quantum process world striving to survive in space and time and this picture is distinct from the particulate and wave views endemic in elementary quantum explanations at present.

RÉSUMÉ. Un mécanisme cellulaire unique, l'automate cellulaire quantique (QCA) est avancé comme le processus candidat a la description de la mécanique quantique fondamentale dans l'espace et le temps réels. Le QCA utilise un mouvement "Zitterbewegung" issu de l'équation des particules libres de Dirac pour les fermions et un treillis d'espace-temps confiné. Il apparaît grâce a l'emploi de regles de calcul de QCA simples qu'une série de processus autopoiétiques (auto formants), d'une certaine échelle peut etre utilisée pour décrire divers états comme les atomes, les noyaux et les particules élémentaires quand ils sont calibrés a 3+1 D états. Les fonctionnalités fractales associeés au QCA font deviner un lien intime entre les propriétés chaos/fractales et les efforts fondamentaux pour comprendre les racines de la physique quantique dans le temps et

* Author to whom all correspondence should be directed.

l'espace réels. Le QCA décrit un monde de processus quantiques luttant pour survivre dans l'espace et le temps réels, et cette description est distincte des points de vue basés sur des particules et des ondes aujourd'hui endémiques dans les explications quantiques élémentaires.

1. Introduction :

Atoms, nuclei and elementary particles seem to have pronounced kinship relationships with one another across spatial scaling barriers. For example these material structures all consist of spin $= \frac{1}{2}$ fermionic matter fields (electrons, protons, neutrons, or quarks) mediated by spin 0 or 1 bosonic fields (photons, pions, gluons, W-particles, etc.)[1]. When using structuralist paradigms to analyze such underlying processes two features dominate the physicist's thinking. First, these systems obey quantum mechanics. Their particle content must have a self interference feature if it is to succumb to quantum real space-time behavior patterns. Secondly, a surviving structured process must vary in a globally coherent fashion such that its constituent parts communicate non-locally with each other.

A fledgling picture of quantum mechanics, the quantum cellular automaton (QCA) incorporates the two features mentioned above in its very postulates[2, 3]. The QCA uses a quantized real space-time lattice similar to the fenced world (*gitterwelt*) described by Heisenberg more than half a century ago[4]. In this world the QCA undergoes *Zitterbewegung*, a quiver motion in all three orthogonal directions at the speed of light predicted quantitatively in the Dirac equation[5]. In this paper we show that such a QCA produces archetypal real space-time structures resulting from autopoietic (self forming) processes based on the zitterbewegung motion, and we apply this QCA behavior to the cases of atoms, nuclei and hadronic elementary particles[5].

Section 2 of this paper defines the QCA in 1+1, 2+1, and 3+1 dimensions and illustrates its salient features where the +1-D designation specifies a freedom in time.

Section 3 defines and develops the fractal dimension **d** of several of the surviving sets of QCAs, which is distinct from the topological dimension **D**. Certain generalizations emerge which relate the fractal dimension of a particular QCA process to specific angular momentum states and represent a novel view of a quantum-fractal interface. Section 4 briefly scales the resulting QCA processes to the world of atoms, nuclei and elementary particles. Novel correspondences can be noted between the QCA properties and physical parameters such as elementary particle mass values, cosmic abundances of nuclei and atomic angular momentum states.

In section 5 a case is made for a strong correspondence between the behavior of the QCA and basic quantum physics. The notion of an autopoietic (Greek: *auto-poiesis = self-forming*) process is advanced here and speculations on future developments of such views are forwarded. The paper concludes in section 6 with a case being made for the QCA process view serving as an imaging mode in real space-time for quantum physics as well as providing several innovative insights on physical states of matter at specific scales.

2. Quantum Cellular Automaton (QCA) Defined

The Quantum Cellular Automaton (QCA) developed previously [2] models an entity or process obeying the Dirac free particle equation, which is valid for any fermion or fractional spin $(\frac{1}{2}, \frac{3}{2}, \frac{5}{2}, ...)$ particle. One of the results of this equation is that the QCA has a microscopic velocity **c** in all three directions and this is the famous *zitterbewegung* (German: *quiver motion*) described originally by Schrodinger[6]. The 1+1 D QCA (one dimension in space and one dimension in time) is defined via the following equation:

$$A(x,t) = A(x-1,t-1) + A(x+1,t-1) \mod 2 \tag{1}$$

where $A(x,t)$ is the value of cell x at time t. The QCA obeying (1) is confined in one spatial dimension box of length $L = Nx_o$ where N is an integer and x_o is half the Compton wavelength of the particle/entity, $\lambda/2 = \hbar/2mc = x_0 = c\tau_o$($\hbar$= Planck's constant divided by 2π and **m** is the mass associated with the process/automaton). Equation (1) can be viewed as a diffusion equation where A(x,t) can take only the values **0**, or **1**. The value of the quantized space-time dimensions were borrowed from Heisenberg who quantized both space and time in his lattice world model[4]. These features are then combined with the notion of the Compton wavelength as being the smallest confinement for a de Broglie wave, x_o being the smallest de Broglie half wavelength[7].

A boundary condition of the form

$$A(1,t) = A(2,t-1) \quad \text{and} \quad A(N,t) = A(N-1,t-1) \tag{2}$$

specifies the behavior of the automaton at the edges of the confining box and becomes a necessary QCA feature. In the above equations both x and t are quantized, $x = rx_o$ and $t = s\tau_o$ with r and s being integers but for convenience only x and t are explicitly mentioned in equations. A provisional initial seeding condition is chosen of the form

$$A\{\text{int}[(N+1)/2], 0\} = 1 \tag{3}$$

where int{} is the integer function, with all other cells assigned a value of 0. In 2+1 D and 3+1 D equations and boundary conditions are similar to (1) and (2) with

$$v_x = v_y = v_z = \pm\mathbf{c} \tag{4}$$

being the necessary QCA requirement. The automaton must move one unit of space diagonally with $\mathbf{x_o} = \mathbf{y_o} = \mathbf{z_o}$ in each unit of time,τ_o in 3+1 D.

The 1+1 D QCA is displayed in Figure 1 for a confinement where $L = 6\mathbf{x_o}$. As can be seen from viewing Figure 1, given the initial seeding condition (3) and the boundary condition (2), **a unique surviving trajectory** emerges in space and time with a recurrence cycle of **k**=14 (the QCA repeats its expression in a $14\tau_o$ time interval). The **1**s not lying on the unique trajectory are on tracks that soon collapse and can be viewed as virtual **1**s which communicate the boundary to the QCA. Every even N-valued QCA yields a single unique surviving space-time trajectory when initially seeded in a single cell. In cases where $N = 2^p - 1$, where p is an integer, the QCA quenches to 0. All N = odd integer values can quench with suitable initial conditions. So for all cases of interest we will only consider lower lying even N-values. In addition, several of the even N-values are ergodic in that they utilize all possible configurations of 1s and 0s over a single recurrence cycle. Ergodic N-values are 2, 4, 6, 10, 12, 18, ... and to date no reliable predictor of which N-values are ergodic has been determined.

Figure 2 shows a typical QCA in 2+1 D for $N^2 = 6^2$. The effects of diverse initial seedings are displayed by means of the shaded cells in 2 a), b), c), d), e), f), g) and h). Unique trajectories appear in all cases with 2a) and 2b) displaying a diagonal trajectory while the six others display closed-path trajectories. Each trajectory can be characterized by an enclosed area **A** and a rotation sense (which is considered + into the paper and - if out of the paper using the right hand rule). Thus 2a) has **A**=0, 2c) has **A**=+8, and 2d) has **A**=-8 as illustrative examples.

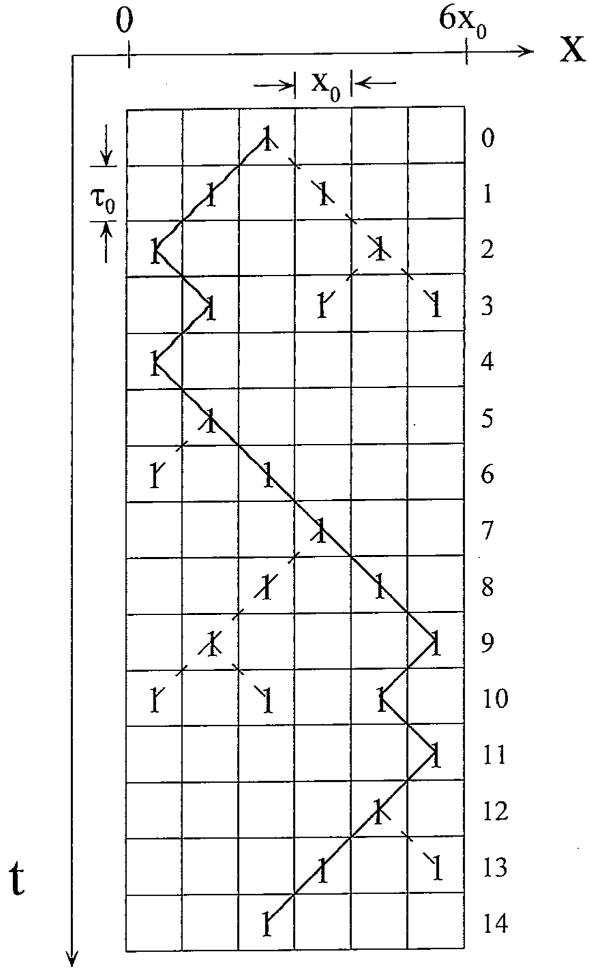

Figure 1. 1+1 D QCA for $N = 6$. All blank cells have a value of **0**. x_0 is the cell width (equal to half the Compton wavelength) and τ_0 is one time step. The initial distribution of **1**s **0**s is reproduced after 14 time steps, a quantity defined as the recurrence time k. The **1** in cell 3 at the recurrence time can be connected backwards in time with the **1** in cell 3 at the initial time through *only one* path, the unique space-time path, indicated by the solid line. The paths represented by the dashed lines do not survive.

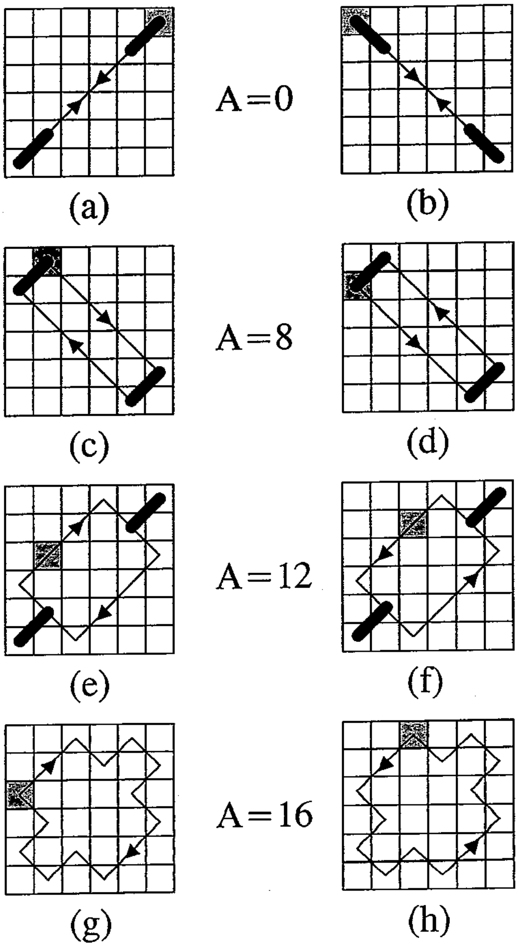

Figure 2. 2+1 D QCAs for $N^2 = 6^2$ displaying different unique trajectory structures which form according to the location of the initial seed. The shaded cell indicates the initial seed, and the magnitude of the area enclosed by the trajectory is indicated for each case. The sense of circulation is indicated by the arrows. The thick segments of the trajectories in (a)-(e) represent the occurence of a back and forth "zitter" before the QCA continues in the direction shown by the arrows.

Antimatter type states eliminate half of the allowed trajectories since the

Dirac equation, the equation the QCA mimics in its behavior, predicts antimatter states being equally likely. Thus if 2a) is considered a matter state, 2b) would have to be an antimatter state since no common cells are occupied in each of these trajectories. Figures 2c) and 2d) would both be matter states since their trajectories occupy the same cells as 2a). A series of 2+1 D features with distinct values for area and a twofold rotation sense hint at a rich variety of "anyon" type structures which have been proposed to model some observed 2D structural features[8].

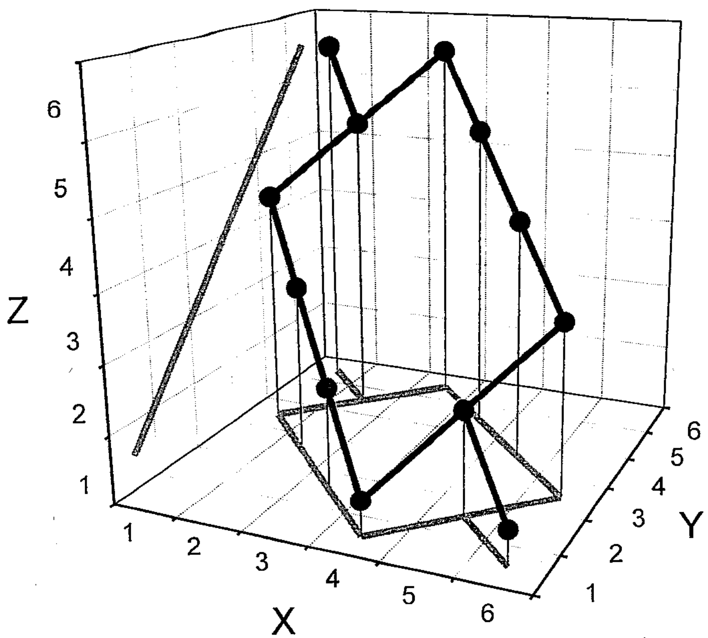

Figure 3. 3+1 D QCA for $N^3 = 6^3$ showing a selected unique planar space trajectory. To aid the reader in visualizing the 3D orientation, the projections of this structure are shown on the xy and yz planes. This particular trajectory is considered a hybrid (see text for details). The component projected on the xy plane has a circulation sense and its shape is identical to that of the $2+1$ D trajectories shown in (e) and (f) of Fig. 2. The recurrence time k is 14.

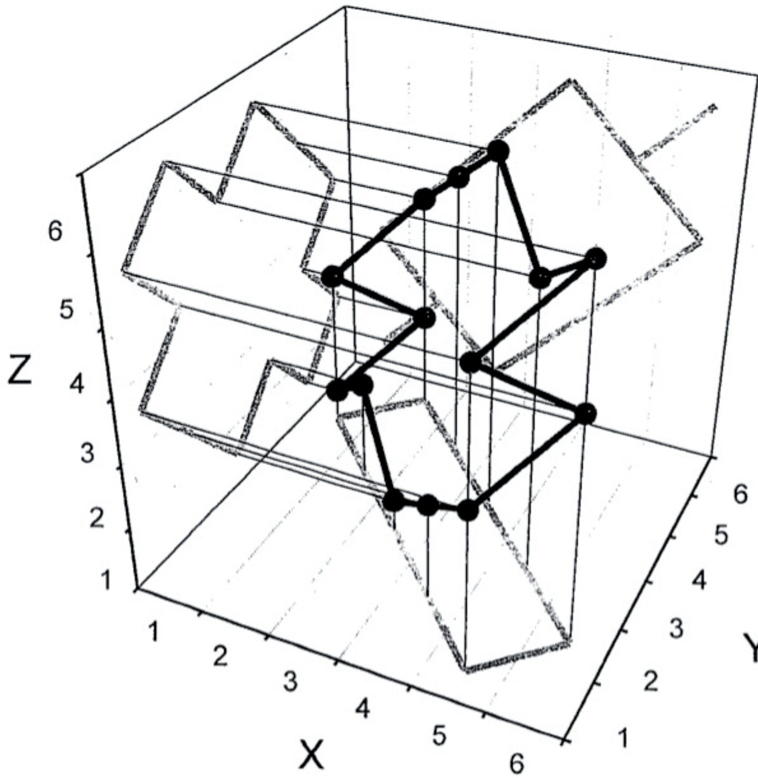

Figure 4. 3+1 D QCA for $N^3 = 6^3$ showing a selected unique non-planar space trajectory. The projections shown display each of the circulating 2+1 D closed trajectories of Fig. 2. As in Fig. 3, $k = 14$.

Figures 3 and 4 display some of the allowed trajectories for the 3+1 D cases with $N^3 = 6^3$. In each of the cases shown unique trajectories are effectively self formed by the QCA rule (1), and the boundary conditions (2), and the initial seeding (3). (The virtual **1**s are not shown in Figures 3 and 4 for clarity of display). The projections of the selected non-planar trajectory shown in Figure 4 show it as a composite of planar orbits identical to those in 2+1 D in Figure 2.

For ease in presentation only N=6 values were illustrated in Figures 1, 2, 3, and 4. Higher N-values continue yielding unique trajectories with distinct **A**-values and distinct rotation senses. For a given N, recursion times, **k**-values, stay the same as the QCA dimension is increased from 1 to 2 to 3.

3. Fractal Features of the QCA

As $N \to \infty$, the fractal dimension $\mathbf{d}$ for the 1+1 D QCA approaches 1.58, the same as the Sierpinski gasket[2]. This motivates the specification of a fractal dimension to all QCA configurations. It is easy to define the QCA fractal dimension via the box counting technique, which can be performed in each case[9]. Thus we define the QCA fractal dimension $\mathbf{d}$ as

$$\mathbf{d} = \ln(\text{total \# of 1s per k time steps})/\ln k \tag{5}$$

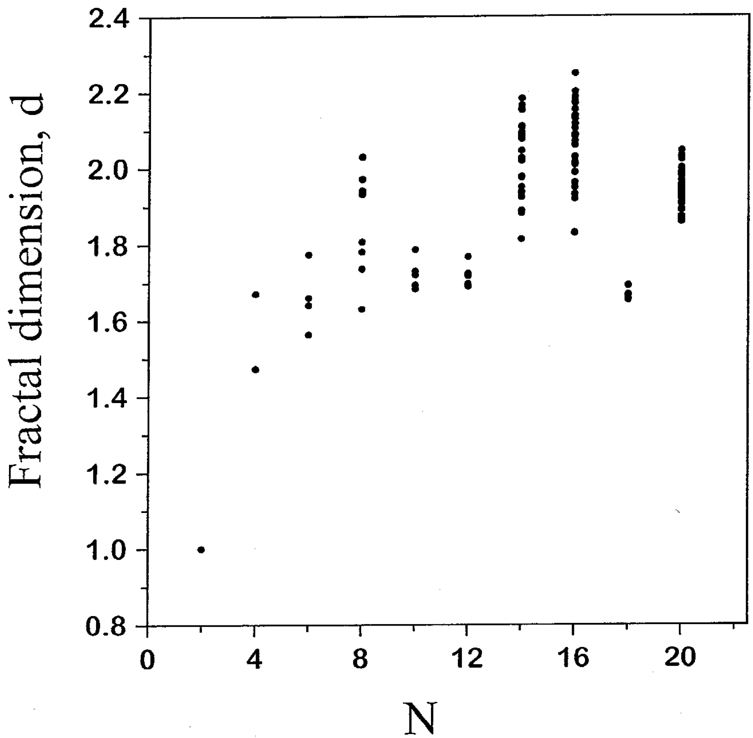

Figure 5. Fractal dimension d of 3+1 D QCA unique space trajectories vs. box size. Different structural trajectories, as a result of varying initial seed, produce the spread in d values for a given box size.

Figure 5 shows a plot of the various d-values as a function of N for the 3+1 D QCA. The scatter of points for a given N-value is a result of different unique trajectories, resulting from different initial seeding conditions which have different fractal dimensions. A closer examination of the unique trajectories shows that *the higher the fractal dimension the smaller the area A* of the closed orbit. In previous work[3] the A-values were shown to be proportional to the angular momentum l, and the N-value was identified with the energy quantum number $n = N/2$ in the case of the hydrogen atom. Thus the $l = 0$ s-states have the largest fractal dimension and the p-, d-, or f-states each have lower values in descending order for a given N-value. This implies that for the relatively low l-states a relatively large number of virtual **1**s communicate the boundary in all directions to a maximal extent, while the high l-states have relatively fewer 1s communicating the boundary. That the $l = 0$ or s-states have relatively high fractal dimensions is consistent with naive orbital models in quantum mechanics where the probability of finding an electron, for example in the s-state of the hydrogen atom, is spherically symmetric even though there can be no net circulation in its orbit. A relationship where $\mathbf{d} =\approx l^{-1}$ would seem plausible although at present the explicit dependence is not tractable.

The ergodic N-values such as 2, 4, 6, 10, 12, 18, . . . as a whole tend to have relatively low **d**-values and a relatively low divergence in these same values when compared to non-ergodic N-values such as N=8 and 14. QCA configurations in N=8 case have the same **k**-value as N=6 but a set of appreciably larger-valued fractal dimensions and a broader range of **d**-values as can be seen from Figure 5. A hypothesis can be advanced that the ergodic QCA states would be more stable than the non-ergodic states, and this can be examined when physical systems are considered in evaluating the efficacy of the QCA model. For example, the QCA might provide an explanation why excited hydrogen energy states always decay with highest probability to the ground state: the $l = 0$ s-state always has the maximum relative fractal dimension. Coherent physical states might exist close to the edge of chaos, chaos being defined here with a high fractal dimension approaching the topological spatial dimension.

These results indicate that quantum physics and fractal physics may indeed have an intimate correspondence. The QCA is one of the few models which brings such relations into focus and the results obtained here should lead to future quantum/fractal developments.

The key feature which adds some theoretical compulsion to the fractal/quantum identification is the strong interference implied by the mod

2 restraint in (1). Viewing a temporal development of the **1**s and **0**s over a recurrence cycle shows a series of buildups of **1**s and periodic collapses often to a single cell, but ultimately the QCA survives. Such variations, the **1**s not lying on the unique trajectories can be considered to be virtual states, can be viewed as a displayable model in real space-time of what a quantum system looks like. The fact that 1+1, 2+1 and 3+1 D confinements have the same recurrence value, **k** for a given N makes the QCA modeling highly tractable.

Poincaré showed almost a century ago that all classical dynamical systems could ultimately be chaotic[10]. In QCA terms they would have a high fractal dimension **d**. It is quantum mechanics and ultimately nature's precision in determining which makes all surviving structures in nature stable. We move now to a few such quantum processes which buttress structural stability in our physical world.

4. Archetypal Scaling of the QCA

A real mystery which is rooted in the foundations of quantum field theory is the role of the unitless fine structure constant, $\alpha(= e^2/\hbar c = 1/137)$. A most remarkable occurrence in physics is that the Bohr radius of the hydrogen atom a_o is 137 times larger than the Compton wavelength λ_c and this latter value is in turn 137 larger than the classical electron radius $\mathbf{r}_c(= e^2/mc^2)$. The classical electron radius can be used as a convenient spatial scale for the world of nuclei and elementary particles as it is about twice the Yukawa wavelength of the pions. The Bohr radius scales atomic spatial confines. The Compton wavelength of the electron is the spatial scale of the QCA and represents an intermediate spatial regime between the world of atoms and the elementary particle and nuclear worlds.

Can the world of atoms, nuclei and elementary particles be reached by scaling the QCA confines spatially upward by a factor of 137 for atoms and downward by this same factor to reach the confines of nuclei and elementary particles? Implied here, of course, would be a feature that the large scale atomic world would have a dynamics 137 times slower than the speed of light and perhaps the particle/nuclear world could have superluminal speeds. From atomic theory we find that the velocity of the electron in the first Bohr orbit is indeed $\mathbf{c}/137$. These are the spatial scales we presently investigate using the QCA paradigms.

Fermionic behavior in real space-time plays a pivotal role in atoms, nuclei and elementary particles. We can assume that electrons in atoms, protons and neutrons in nuclei and the quarks in elementary particles are all spin $\frac{1}{2}$ fermions and thus subservient to the Dirac free particle equation when weakly bound. We consider each of these three distinct systems in turn.

To initiate the scaling considerations at the atomic scale we offer Table 1 which lists the number of allowed trajectories for each N-value up to N=6. Each unique trajectory can be considered a state into which suitable fermions can be fitted. The number of allowed trajectories are halved in the fourth column of Table 1 since we count only matter states. In the non-planar orbits displayed earlier in Figure 4 there is an additional twofold degeneracy since in that case each one of the 12 allowed orbital states shares the same 3-D confines as one of the others.

Table 1: Synopsis of $3+1$ D QCA properties

Box Size (N_3)	Area A	Recursion ($\mathbf{k}$)	# of Unique Trajectories	orbital Match
2	0	2	(4)2	1s
4	0	6	(4)2	2S
	6	6	(12)6	2p
6	0	14	(4)2	3s
	12	14	(12)6	3p
	18	14	(12)6	3sd
	18	14	(24)6/12 non-planar	3spd
	24	14	(12)6	3d

a. Atoms

If we start with hydrogen we can assert that the electron is bound with a maximum energy of 13.6 eV while its rest mass is about 0.511 MeV/c^2, an energy ratio of 1 to 40,000. With such a miniscule binding to rest mass energy ratio the orbiting electron is an effectively free particle in the Dirac equation, making it a candidate QCA process. Since each

QCA forms its own space and time the lowest energy configuration of such a weakly bound system would be that of the smallest allowable box with N=2.

In previous work[3], the following QCA features were shown to emerge:

1. The energy quantum number n in the simpler cases can be identified with N/2

2. The angular momentum quantum number l has a correspondence to the area **A** of a unique trajectory as shown in Figures 3 and 4.

3. The magnetic quantum number m_l corresponds to the inclination of a unique trajectory and its spin quantum number corresponds to its rotation sense, + or -.

4. The electron has no "intrinsic" spin but its spin quantum number s is the result of *Zitterbewegung* as shown previously for the QCA case[3] and by several other authors[11].

The number of electrons in each orbit closely corresponds to the number of unique trajectories allowed for the QCA up to N=6 or $n = 3$. For higher N-values counting techniques can be implemented which at present are still unclear but show promise.

b. Nuclei

The proton and neutron, each of which are fermions with spin = $\frac{1}{2}$, and a mass of about 940 MeV/c^2 are bound in a typical nucleus with an energy of about 10 MeV which is about a 100 to 1 rest energy to binding energy making these nucleons somewhat free particles and thus QCA candidates. We can now count nuclear states corresponding to QCA unique trajectories.

With N=2 only two unique trajectories are allowed. Here we can assert that either two protons or two neutrons can fill this state thus making a total nucleon number of 4 which corresponds to Helium-4. At N=4 we have 2+6 = 8 allowable states which again would correspond to Oxygen-16, 8 protons and 8 neutrons. In the nuclear counting procedure we do not count inner shells filling prior to outer shells but rather just count the states allowable in a given shell.

Proceeding further to N=6 we have a total of 2+6+6+6+12 = 32 distinct planes allowable but the 12 non-planar trajectories can be reduced to two pairs of 6 each which occupy identical volumes. We have a total of 26 unique trajectories to fill which would yield Iron with 26 protons and 26 neutrons. Iron-52 is not stable but Iron-56 at 92% abundance and Iron-54 at 6% are Iron's most abundant isotopes[12]. Counting QCA states to match nuclear abundances yields no clear outcome. New neutron counting techniques seem to be called for to match nature's nuclear count.

QCA counting yields a new set of "magic" numbers namely 2, 8, 26, 52, etc. which are distinct from the older set of 2, 8, 20, 50, etc. The QCA counting at least hints that Iron with its 26 protons should be a relatively popular nuclear species as indeed it is in nature.

c. Elementary Particles

The standard model of quantum chromodynamics (QCD) in its simpler version would have all massive elementary particles composed of a combination of spin = 1/2 quarks that undergo some sort of dynamics in the particle's innards. Irrespective of the binding energies of such fermionic constituents and the unknown quark rest masses it should be instructive to examine such dynamics in terms of the QCA model.

Another important physical feature of the composite particle is its inertial mass and it is here we can gain some insight on such particles vis-a-vis QCA dynamics. Inertial mass can be considered a quantification of a lingering in a local region of the confined box. If the particle described by the QCA in Figure 1 were of low mass its unique trajectory should bounce back and forth from one bound extreme to the other in a minimum amount of time. The more massive particles would experience a longer recursion time, **k**.

Using Bohm's version of the uncertainty relation[13] we can write the particle's diffusion by the equation

$$(\Delta\times)^2 >= (\hbar/m)(\Delta t) \tag{6}$$

If we now solve the above equation for **m**, the mass of the diffusing particle, and consider its diffusion over an entire recursion cycle ($\Delta t = \mathbf{k}\tau_o$) we have

$$\mathbf{m} = \mathbf{k}(\hbar/c)(1/\times_o) \tag{7}$$

which ultimately yields the relation that $\mathbf{m} \approx \mathbf{k}$ since all the other parameters in (7) are constants.

Since the simplest configuration we have is N=2 we can normalize the N=2 QCA as our base mass unit and define a mass ratio as follows

$$\mathbf{m}(N_1)/\mathbf{m}(N_2) = \mathbf{k}_1/\mathbf{k}_2 \tag{8}$$

Table 2 presents a list of recursion values ranging for N=2 to N=12. We can see for example that the masses of the particles described by the N=4 QCA would be 3 times the masses of those described by the N=2 QCA. Further the mass described by the N=6 QCA would be 7 times those masses of the N=2 process.

Table 2: Recursion **k**-values for 2 <= N <=12

N	**k**
2	2
4	6
6	14
8	14
10	62
12	126

There is both experimental[14] and theoretical[15] evidence that the pions, the lightest scalar spin 0 mesons, would be the likely hadronic candidates to occupy the N=2 state. There is a bifurcated pionic mass spectrum, the π^o at 134.97 MeV/c^2 and the charged pions π^+ and π^- at 139.57 MeV/c^2[16]. The π^+ is the antiparticle of the π^- and the π^o is its own antiparticle and so the two allowable matter states with N=2 are then filled. A base mass unit would of necessity be its own antiparticle as is the π^o and in the electropionic models the π^o [15], which is the least massive of all hadrons, is the generator of the QCA mass spectrum via (8).

A summary of the masses generated by (8) at assorted N- values is shown in Table 3 using the pions as mass generators or base mass units.

In Table 3 all identifications are made on the basis of mass alone without spin, charge, or any other isospatial classifications. However based on mass alone it would be suitable to place the Kaons at masses of about 495 MeV/c^2 and perhaps the $\eta(548)$ to fill some of the other

Table 3: Tabulated QCA Electropionic Masses Generated

N	Calculated Mass MeV/c^2	Experimental Mass Candidates [16] MeV/c^2
2	134.97	$\pi^o(134.97)$
	139.57	$\pi^+ - (139.57)$
4	404.91	ε-meson(?) or σ-meson(?)
	418.71	
6	944.79	P(938.27) or N(939.55)
	976.99	$a_o(982.4)$ or $f_o(980)$
		or $\eta'(958)$
8	944.79	P(938.27) or N(939.55
	976.99	$a_o(982.4)$ or $f_o(980)$
		or $\eta'(958)$
10	4184	$\psi(4160)$
	4327	$\psi(4415)$
12	8503	No present candidate
	8793	No present candidate

available sites in the N=4 row as there are six additional states allowed. The prime QCA mass at N=4 ranging from about 405 to 420 MeV/c^2 resonates with the purported presence of the σ or ε mesons which never have been detected experimentally despite their theoretical compulsion in many particle models[17]. As a matter of course these unfound mesons can be viewed as the Higgs mesons of orthodox QCD because without such a mesonic mass there would be no way to generate the light mesons at all.

It would be reasonable to place the baryons, both spin $\frac{1}{2}$ and spin 3/2 varieties, in the stable low fractal **d** N=6 categories. As we know from quark/parton studies there is a pronounced threeness in neutrons and protons and the more stable baryons. The N=6 suggests a pronounced n=3 QCA quantum feature, scaled down from atomic analogies.

The higher base mass units listed for the N=6 and N=8 rows, the a_o and f_o are experimentally very interesting particles when their Kaon decay modes are considered. In the QCA picture there is no difficulty in having N=8 trajectories degenerate to the N=4 level and indeed some of the N=8 modes have identical areas with their N=4 kaonic relatives. All the N=8 sites should be relatively unstable, at least less stable than the N=6 sites, due to their relatively high fractal **d**.

At present no version of QCD can predict or even retrodict the masses of particles. The masses of the quarks, if they have much mass at all, are adjusted and manipulated in various aspects of QCD to save various mechanisms. The QCA archetypal process view lacks precision at present in explaining atomic, nuclear and elementary particle parameters clearly. However there are remarkably familiar glimpses of some spiraculous processes which have appeared in other more orthodox formulations suggesting identical features at these levels of matter.

If we persist in ultimate atomistic views of matter over the autopoiesis of the QCA we will be forced to introduce new rubrics of behavior via recondite algebras and hidden symmetries as we encounter each new level in the future. At the Planck length, $[G\hbar/c^3]^{\frac{1}{2}} = 2 \times 10^{-35}$ meter, ultimate atomism sees all reality and its theories behaving the same way[18]. In this autopoietic view the same behavioral process prevails for a few modest scales of 137 in space and time rather than the 10^{20} needed to get to the Planck length.

5. QCA Quantum Views

There are many active and diverse interpretations of quantum mechanics in the physics of the day[19]. Paradoxes, problems and a whole series of unanswered but crucial questions remain unresolved in all quantum foundational models[20]. The QCA picture provides some new insights which resonate with some outcomes of other older views.

If one starts with the Heisenberg uncertainty relations

$$\Delta \times \Delta \mathbf{p} >= \hbar \quad \text{and} \quad \Delta \mathbf{E} \Delta t >= \hbar \tag{9}$$

where **p** and **E** are the momentum and energy of a given particle or process it is a matter of preference whether one quantizes momentum or space, energy or time. Heisenberg used the *gitterwelt* (fenced world or lattice world) idea in early attempts to fathom the depths of quantum behavior in space and time[4]. The QCA represents a continuation of such attempts.

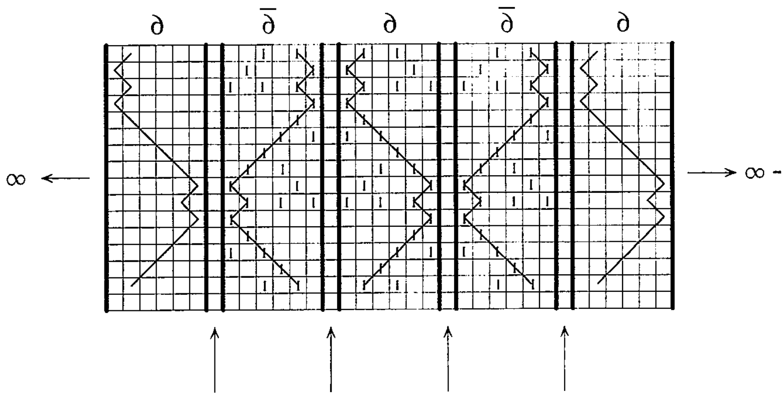

Figure 6. Simulated boundary conditions consistent with QCA rules in 1+1 D for $N = 6$. The nested QCA is in the center. The arrows indicate where the boundary interference occurs.

The boundary feature of the QCA in (2) is an essential QCA feature which deserves more attention. The boundary condition represented in (2) can be achieved by having another QCA provide destructive interference at the box edges. Figure 6 shows how the boundary cancellation can occur in the 1+1 D case where N=6. The cancellation can occur only if another QCA operates 180^o out of phase and adjacent to the original, thus making it an antimatter QCA which for convenience we represent as $\bar{\mathbf{6}}$. All the cells occupied by each of the **1**s in $\bar{\mathbf{6}}$ are vacant in **6** at the same time interval. This means we can invoke boundary conditions by using QCA processes without imposing another structure or construct such as a potential, reflecting mechanism, or virtual particle exchanges as is often done in traditional quantum theory.

Thus each process confined via (2) can be considered as being nested in a surrounding medium, no longer a vacuum state, which is filled with a series of **6**s and $\bar{\mathbf{6}}$s alternating towards infinity in each direction as shown in Figure 6. The same features can be employed in 2+1 D and 3+1 D to confine the QCA process. This would mean that as a quantum process each QCA is surrounded by a plenum of matter/antimatter processes alternately ordered to the extremities of the universe. Notions of quantum tunneling can be easily understood in such a version. No barrier need be penetrated by a particle as in conventional views which would mean that the "external field," which is usually viewed as confining mechanism in such a process, is in reality a series of **6** $\bar{\mathbf{6}}$ QCA processes similar to that shown in Figure 6.

The problem of quantum measurement was discussed in previous QCA papers [2,3] and the unique proviso emerging in this view is that all measurements must be made going backwards in time. The unique trajectory as displayed in Figures 1 through 4 cannot be determined locally but only by proceeding backwards in time over at least one recurrence cycle. There is no way for a **1** in any given cell to determine if it is to survive by being on the unique trajectory. The instantaneous collapse of the wave function often associated with measurements corresponds to a collapse of virtual **1**s in the QCA picture.

Quantum mechanics ultimately describes physical processes and not the migration of little billiard balls or localized packets of energy and momentum in a surrounding void irrespective of the spatial extent of its confines. The particle/packet models are forced to borrow much of their interesting physics from the recondite vacuum mechanisms that proliferate the physics of many modern formulations. The quantum chromodynamics (QCD) vacuum is emerging as the most fertile, imaginative and interesting physical study of the modern era[21]. Vacuum mechanism invention is becoming the bastion of modern field theoretic practices.

The QCA view thus gives a unique insight on confinement problems, some aspects of the measurement problems and perhaps hints at the presence of pilot waves as expressed by the virtual **1**s, all of which are persistent in various quantum formulations.

6. Conclusion

Quantum mechanics describes processes in real space and real time. The QCA is a fenced world of space and time. Anaximander had his original state of the universe be *apeiron*(the unbounded) at the very beginnings of scientific thought[22]. He also had his matter tidbits undergoing eternal motion. Once this process became bounded, ordered reality came to be. The QCA fulfills Anaximander's insight some 2500 years later. However each tidbit of this universe is counting and calculating its future existence as it struggles to survive.

The QCA also behaves in a manner similar to the monads Leibnitz proposed three centuries ago[23]. In the monadic view matter was not inert and dead but had innate eternal motion. Each monad makes its own space and its own time and has a miniscule perception of the entire universe. Leibnitz was criticized for giving matter a soul or putting a God of pure act in the innards of matter. Physics for centuries neglected this view and became more comfortable with external forces manipulating the dead and inert matter of today's particles into its many forms. What the QCA view resurrects, which also is the insight provided by quantum theory, is the notion that indeed all processes we identify as material are seething and striving to survive, having luminal dynamical processes embedded in their internal structure. These processes are essentially distinguished only by scale. The QCA world is one of calculating, self-interfering and self-forming its recurring survival processes that become stable dynamical structures in real space-time.

References

[1] C. Rubbia, *The Quest for the Infinitely Small*, Il Nuovo Cimento **197A**, 1001-1044(1994).

[2] D. Belousek, E. Hinigan, D. Hott and J.Kenny, *Quantum Cellular Automaton in 1-D*, Chaos, Solitons and Fractals **4**, 439- 460(1994) and D. Belousek, N. Clements, L. Goodman and J. Kenny, *Quantum Automaton in a 1-D box*, Chaos, Solitons and Fractals **2**, 661-673(1992).

[3] D. Belousek, E. Flint, J. Kenny and K. Roos, *A QCA in 2+1 and 3+1 Dimensions*, Chaos, Solitons and Fractals **7**, 853 (1996).

[4] W. Heisenberg, *Die Selbstenergie der Elektrons*, Z. fur Physik **65**, 4-13(1930) and B. Carazza and H. Kragh, *Heisenberg's lattice world: The 1930 theory sketch*, American Journal of Physics **63**, 595-605(1995).

[5] P. A. M. Dirac, Principles of Quantum Mechanics (4^{th} Ed.), Oxford U. Press (1958) and P.A.M. Dirac, Proceedings of the Royal Society **A117**, 610(1928)

[6] E. Schrodinger, *Sitzung sb. Preuss Akad. Wiss.* Phys. Math. **24**, 418(1930).

[7] L. de Broglie, *Recherches sur la theorie des quanta*, Annales de Physique **3**, 22-128(1925).

[8] L. J. Challis, *Physics in less than three dimensions*, Contemporary Physics **33**, 111-127(1993)

[9] H. O. Pietgen, H. Jurgens and D. Saupe, Chaos and Fractals: New Frontiers of Science, Springer-Verlag, New York (1992), pp. 24- 30.

[10] J. H. Poincare, Les Methodes Nouvelle de la Mechanique Celeste, Gauthier-Viller, Paris (1892).

[11] K. Huang, *On the Zitterbewegung of the Dirac Electron*, American Journal of Physics **20**, 479-84(1942) and Hans Ohanian, *What is Spin?*, American Journal of Physics **54**, 500-505(1980).

[12] A. H. Wapstra and K. Bos, Atomic Data and Nuclear Data Tables **19**, 175(1977).
[13] D. Bohm and Basil J. Hiley, *The de Broglie pilot wave and other insights arising out of it*, Foundations of Physics **12**, 1001- 1016(1982).
[14] M. MacGregor, *Can 35 Pionic Mass Intervals among Related Resonances be Accidental?*, Il Nuovo Cimento **58A**, 159- 180(1980).
[15] J. Kenny, *An E/M Inertial Mass Theory Applied to Elementary Particles*, Int. Journal of Theoretical Physics **13**, 341-360(1975) and J. Kenny, *Electropionics and Fusion*, Fusion Technology **19**, 547-551(1991).
[16] Particle D Group, *Review of Particle Properties*, Physical Review **D50**, 1173-1826(1994).
[17] N. A. Tornquist and Matts Roos, *Confinement of the σ-meson*, Physical Review Letters **76**, 1575-1578(1996).
[18] E. R. Harrison, Cosmology: The Science of the Universe, Cambridge Univ. Press (1991), pp. 329-345.
[19] S. Sonego, *Conceptual foundations of quantum theory: a map of the land*, Ann. De la Fond. Louis de Broglie **17**, 405-478(1992).
[20] M. Surdin,*Essai de reponse a quelques questions*, Ann. De la Fond. Louis de Broglie **19**, 173-201(1994).
[21] G. Preparata, *Hadron'93: Theory*, Il Nuovo Cimento **107A**, 2657- 71 (1994).
[22] M. Hesse, Forces and Fields, Littlefield, Adams (1975), p. 39.
[23] G. W. Leibnitz, Discourse on Metaphysics, Correspondence with Arnaud and Metaphysics, (English translation), Open Court Press, LaSalle, Illinois (1980), pp. 252-272.

(Manuscrit reçu le 16 avril 1996)